2011 American Control Conference
on O'Farrell Street, San Francisco, CA, USA
June 29 - July 01, 2011

Iterative Learning Control of a Camless Valve Actuation System with Internal Feedback

Adam Heinzen, Pradeep Gillella, and Zongxuan Sun
Department of Mechanical Engineering
University of Minnesota, Twin Cities
Minneapolis, MN 55455, USA

Abstract— **This paper presents the iterative learning control of an electro-hydraulic fully flexible engine valve actuation system. The specific camless system has a unique hydro-mechanical feedback mechanism that simplifies the external control to the choice of triggering timings for three two-state valves. All the critical parameters describing the engine valve event, i.e. lift, duration, timing, and seating velocity, can be continuously varied by controlling these timings. Initial testing of a prototype experimental setup reveals that the performance of the system (transient tracking and steady-state variability) is influenced purely by the state of the system when the internal feedback mechanism is activated. This feature, along with the cyclic nature of the engine valve operation, motivates the development of a iterative-learning-based feedback and feed-forward controller to identify and set the optimal operating point in real time using the output of the previous cycle and the desired performance. The learning control implementation presented here is unique in that, instead of calculating a control signal (sequence) for each cycle, it sets the triggering timings for each of the on-off valves, which directly affect the initial conditions for the internal feedback loop. Experimental results demonstrate that the controller is able to minimize lift and closing time errors while satisfying the seating velocity constraint even during aggressive transient operation.**

I. Introduction

Internal combustion engines (ICEs) are the preferred power source for many applications, including automobiles, locomotives, ships, and electric generators, due to their power density as well as the high energy density of the hydrocarbon fuels they typically burn. Concerns associated with ICEs include the dwindling supply of fossil fuels and greenhouse gas emissions. Thus, there is a strong motivation to increase the efficiency of the ICE.

More flexibility in available controls will allow the engine to operate near peak efficiency more of the time. One such flexibility that can provide many advantages in efficiency and emissions is variable valve actuation. The vast majority of reciprocating ICEs (the most common type) use one or more camshafts with eccentric lobes to actuate the intake and exhaust valves that control the flow of air, fuel, and combustion products in and out of the cylinders. However, the fixed geometry of these cams means that the valve lift profiles for the engine are fixed irrespective of load, engine speed, or any other potentially relevant variables. Variable-valve actuation schemes utilizing cams have been implemented allowing two discrete camshaft profiles [1], and variable phasing and lift [2], to list two examples. However, the use of the camshaft imposes limits on the range of variability of lift and phasing, and makes independent duration adjustment difficult. These systems also exhibit increasing mechanical complexity with increasing flexibility.

Fully-flexible valve actuation (FFVA) or "camless" systems allow infinite variation of lift, timing, and duration over a wide range. This flexibility has advantages in efficiency and emissions. It facilitates cylinder deactivation [3], throttle-less operation [2], [4], [5], changing the engine's effective compression ratio via late- and early-IVC strategies [4], [6], and the control of homogeneous-charge compression ignition (HCCI) [6]. A more rigorous discussion on the benefits of flexibility in valve actuation can be found in [2]-[6].

Most previous FFVA implementations, for example [7], [8], are based on the use of complex feedback controllers to monitor the valve's position in real time and calculate the appropriate control action for the actuator. This approach demands accurate, low-noise position sensors and powerful microprocessors to enable low-latency, real-time calculation of the control effort. In addition, accurate and high-bandwidth actuators are needed to control the valve to the desired position, even at high engine speeds. As such, this strategy may be expensive and difficult to implement on a production engine.

A production-oriented camless FFVA system is required to operate with the same level of accuracy and repeatability when compared to existing cam-based systems to ensure proper engine operation and to avoid piston-valve interference. Such a system is also required to be relatively inexpensive to manufacture while having a sufficient bandwidth to allow high-speed engine operation. To ensure accurate valve positioning, repeatability, and robustness to disturbances, the control system must be suited for mass production; i.e., it should use control algorithms capable of operating on the engine's control unit with a relatively low computational burden, low-cost sensors, and should require minimum calibration.

This paper presents the control design for a production-oriented FFVA system based on a hydro-mechanical internal feedback mechanism [9]-[11]. It was observed that, for a given physical design of the new system, its trajectory and consequently the performance parameters corresponding to

Corresponding author :: Zongxuan Sun, zsun@umn.edu, 612-625-2107

978-1-4577-0079-8/11/$26.00 ©2011 AACC

the engine valve event are dependent only on the initial state of the hydro-mechanical internal feedback system (IFS), which can be modified in real time by adjusting the timing of simple two-state valves. However, the initial state of the IFS corresponding to the optimal performance vary with system operating conditions, thus making the use of a calibration-based open-loop controller intractable. This motivates the development of an iterative-learning-based controller capable of modifying the initial state by adjusting the timing of the activation/deactivation of the IFS to achieve the required performance objectives.

The system performance parameters (lift, closing timing and seating velocity) need to be evaluated only once at the end of each cycle. This relaxes the demand for noise-free position sensors and also decreases the computational burden. The control inputs (i.e., the triggering timings for the three two-state valves) need to be computed only once for each engine cycle (at the start of the cycle). The engine valves will be open for about one-fourth to one-third of the engine's 720-crank-angle-degree (CAD) cycle. This reduces the required real-time processing capability, as the actions for the next valve event can be calculated after the current event during the remaining time (approximately 360-480 CAD).

The rest of the paper is organized as follows. A brief description of the system design and operation is first presented. This helps identify some of the performance characteristics and the corresponding control challenges. It is followed by the development of a control strategy to address each of the challenges. The final section presents the performance of a prototype experimental setup to demonstrate the effectiveness of the proposed controller.

II. Electro-Hydraulic Valve Actuation System With Internal Feedback

The concept of the new production-oriented FFVA system based on the internal feedback mechanism was first presented in [10]. [9] addressed some of the design and sizing considerations for the system and also demonstrated the effectiveness of the concept using a prototype experimental setup. [11] presented a mathematical model for the system, which was verified experimentally and used for the design of a critical subsystem to improve the performance and robustness of the system.

A. System Design and Operation

Fig. 1 shows a schematic of the valve actuator with the internal feedback system. The high-pressure rail and the low-pressure reservoir are common to all the actuators. Components $\{1\}$ through $\{5\}$ together constitute the actuator for one engine valve. Component $\{3\}$ is a two-position, three-way solenoid valve, which connects the entire system to the high-pressure rail or the reservoir. Component $\{4\}$ is the spring-returned hydraulic actuator, which is in contact with the engine valve's stem. Component $\{5\}$ is a spool valve, which controls the fluid flow to and from the main actuator chamber (a). It is designed such that the flow rate is maximum when the spool is at the center position and

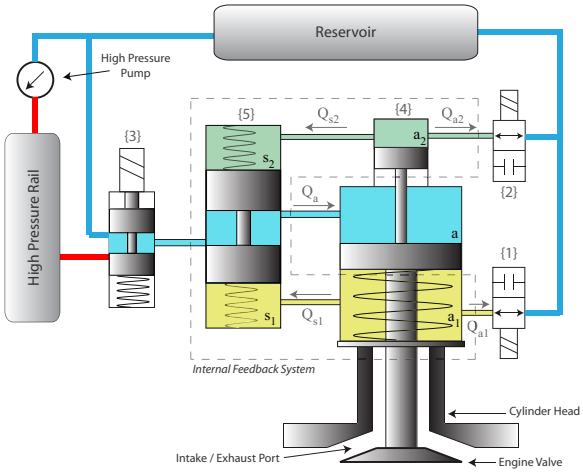

Fig. 1. Schematic of the valve actuation system with internal feedback

decreases when the spool is deflected in either direction. The position of the spool is dependent on the pressure of the fluid in the (s_1) and (s_2) fluid chambers, which are in turn dependent on the pressure in the (a_1) and (a_2) fluid chambers of the actuator. Components $\{1\}$ and $\{2\}$ are two-way, on-off valves that allow or block fluid flow between the actuator's bottom and top fluid chambers, respectively, and the reservoir.

When all the valves $\{1\}$, $\{2\}$, and $\{3\}$ are in the de-energized state, the actuator's main chamber (a) is connected to the reservoir and the spring force keeps the engine valve in the closed position. (s_1), (s_2), (a_1) and (a_2) are all connected to the reservoir. This enables the springs to hold the spool in the middle position, which would allow maximum flow to and from the actuator.

To open the engine valve, the three-way solenoid valve is energized to connect the actuator's main fluid chamber to the high-pressure rail which opens the engine valve. To control the lift of the engine valve, on-off valve $\{1\}$ is closed at a predetermined timing during the actuator's opening stroke. This blocks the flow from (a_1) to the low-pressure reservoir and diverts it to (s_1) of the spool valve, which pushes the spool upwards and hence reduces the flow to the actuator. The decrease in flow gradually decelerates the actuator until it comes to rest at a position corresponding to the fully deflected position of the spool. Fig. 2(a) presents experimental data in which different valve lifts were obtained by varying the relative triggering time of the on-off valve $\{1\}$ with respect to the three-way valve's triggering timing.

To close the engine valve, the three-way valve and the on-off valve $\{1\}$ are both de-energized. The spool in $\{5\}$ returns to the center position and thus connects the actuator's main chamber to the low-pressure reservoir which causes the engine valve to close due to the spring force. During the engine valve's upward motion, the fluid from (a_2) is pushed into the low-pressure reservoir. As the valve approaches the closed position, the on-off valve $\{2\}$ is energized. This diverts the fluid from (a_2) to (s_2). The spool is deflected downwards and hence restricts the flow out of the actuator's main chamber, which in turn decelerates the actuator. By

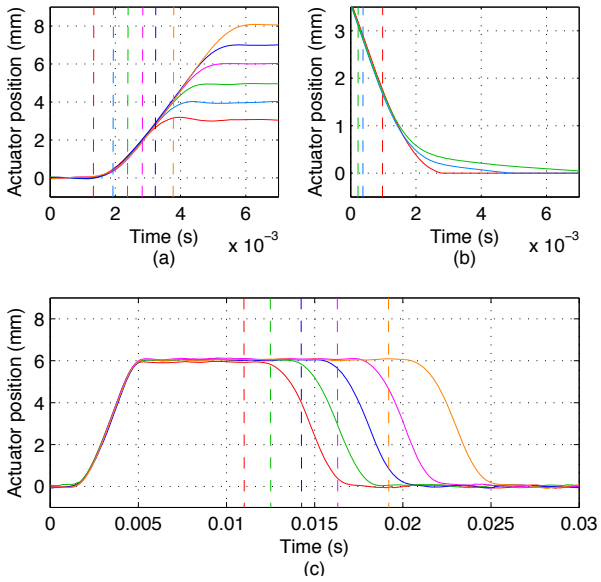

Fig. 2. Experimental demonstration of the variable lift (a), seating velocity (b), and duration (c) control capability of the new valve actuation system. Solid lines represent valve position traces, and dashed lines are valve $\{1\}$ on (a), valve $\{2\}$ on (b), and valve $\{3\}$ off (c) triggering times.

varying the triggering timing of the three-way valve $\{3\}$ and on-off valve $\{2\}$, the engine valve's closing timing and its seating velocity can both be controlled precisely. Fig. 2(b) shows three different seating velocity behaviors obtained by triggering on-off valve $\{2\}$ at different engine valve positions. Fig. 2(c) shows five different valve profiles together with the corresponding three-way valve off timings to demonstrate the ability to control the engine valve's closing timing (duration). Note that in Fig. 2(a) and (c), the three-way valve is turned on at $t = 0$ seconds.

B. System Characteristics and Challenges

From the design and operation of the system, it becomes clear that the choice of triggering timing for the three-way and the on-off valves determines all the valve event characteristics (timing, lift, duration, and seating velocity) for a given cycle. This greatly simplifies the control of the system. When compared to other actuation systems [7], [8] that rely on traditional real-time sample-to-sample feedback control, this architecture requires only that the values for the control inputs (triggering timings) be computed for each cycle.

The on-off valves $\{1\}$ and $\{2\}$ (u_1, u_2) can be triggered either at a predetermined time (CAD) or at a predetermined engine valve displacement to achieve the required performance. Both of these implementations have their own advantages and disadvantages. Triggering based on displacement is inherently robust and requires little calibration, as the engine valve displacement after an on-off valve is triggered is fixed depending on the ratios of piston areas s_1/a_1 and s_2/a_2 (see Fig. 1). This approach also has the advantage of being insensitive to engine speed. However, it requires real-time monitoring of the engine valve's position. This renders filtering the displacement sensor's output unattractive due to the effect of filter delay, which thus requires the use of a higher-cost, lower-noise displacement sensor to ensure accurate triggering. For a fixed triggering position, closing time and seating velocity will vary based on the lift from which the valve is returning (due to variation in velocity at the instant when the on-off valve is triggered).

Triggering based on timing (CAD) allows filtering of displacement data (needed only for performance parameter calculations, which can be performed just before the start of the next cycle). This allows the use of lower-cost displacement sensors and an encoder to measure the crankshaft orientation. However, the triggering timings in CAD will vary with supply pressure, engine speed, and valve lift. A calibration-based open-loop control of the timing for all possible engine valve events and operating conditions would be extremely tedious, if not intractable.

For both schemes, some uncertainty will be present due to the switching times of the on-off valves and hydraulic delays in the IFS circuits. A cycle-to-cycle learning control scheme would be able to find and adjust the timing or displacement at which the control valves are triggered based on the required performance and the operating point of the system. This would allow the system to be robust to changes in engine operating conditions, which are likely to change slowly when compared to the length of the engine cycle.

By the nature of the system, the three-way valve triggering (u_3) must be implemented in the time (or CAD) domain. The controller presented here is designed to utilize either CAD-based triggering or position-based triggering for u_1 and u_2. Experimental results will be presented for a controller that utilizes CAD-based triggering for u_1 and position-based triggering for u_2. Position-based triggering was used for u_2 because it offered superior tracking performance over CAD-based triggering, as it was able to respond to cycle-to-cycle variability in the engine valve's return trajectory. CAD-based triggering was used for u_1 because it offered similar lift tracking performance to position-based triggering, with the additional benefit of allowing u_1 to be activated before the valve's position has moved above the sensor noise level. This facilitates lift capability lower than the approximately 4-mm limit observed with position-based triggering, down to approximately 2.2 mm (in the limit of triggering u_1 in advance of the three-way valve u_3).

III. Controller Design

An iterative learning controller (ILC) was designed to improve the steady-state and transient tracking performance. Traditional iterative learning control modifies the input signal for the current iteration based on the error signals from one or more of the previous iterations. [12] presents a summary of this type of ILC. As discussed in the previous section, the errors for the present controller are not continuous but discrete: the errors in lift, in closing time, and in seating velocity for the past cycle. ILCs have been implemented using a scalar error to build a continuous control signal; [13] contains one such example. In the present system, the inputs to the system are also not continuous signals; they are values

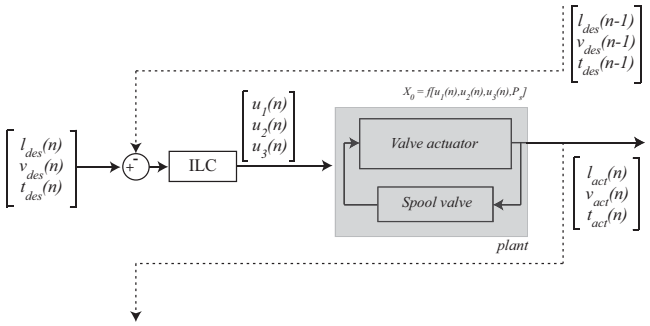

Fig. 3. Block diagram of the proposed iterative learning controller

for the timing for energizing and de-energizing the on-off and three-way valves, which change only once per cycle.

Since the behavior of the plant when the IFS is active is fixed by design, the controller can affect the output only by altering the state of the plant when the feedback is activated. Effectively, the external controller sets the times at which the IFS becomes active, thus setting the initial conditions from which the internal feedback loop will operate. The present external controller is therefore an iterative learning controller for initial conditions of the fixed hydro-mechanical internal feedback mechanism.

Fig. 3 shows a block diagram of the proposed ILC architecture in which the the plant is presented as a feedback structure. A detailed description of the mathematical model, the design parameters, and the analysis of the internal feedback mechanism is presented in [11]. The controller affects the performance of the system by calculating the triggering timings u_1, u_2 and u_3 for the three valves during engine valve opening and closing, which sets the initial conditions (X_0) for all the states of the feedback loop. The output of the plant is then calculated at the end of each cycle. Fig. 4 shows a typical valve position and velocity trace and the corresponding valve event performance parameters. This output is used by the ILC to adjust the control input for the subsequent cycle to achieve the desired performance.

A. Lift controller

Lift is calculated by averaging the actuator's position over the 5 CAD prior to turning off the three-way valve as shown in Fig. 4. This averaging makes the lift measurement more robust to sensor noise. A simple proportional-type learning controller as shown in Eq. (1) is implemented for lift tracking.

$$u_1(n) = u_1(n-1) + K_1 \times [l_{des}(n) - l_{act}(n-1)], \tag{1}$$

where u_1 is the time (in CAD after the opening of the three-way valve) at which on-off valve $\{1\}$ is closed, K_1 is the proportional learning gain and l is the lift (both desired and actual). The indices n and $n-1$ are used to represent the current and previous cycles, respectively. For the CAD-based triggering, K_1 is chosen as $[\Delta l_{act}/\Delta u_1]^{-1}$ CAD/mm where $[\Delta l_{act}/\Delta u_1]$ is the slope of the line approximating the data from open-loop tests relating the triggering timing of u_1 and the valve lift l_{act}. It would also be possible to update this

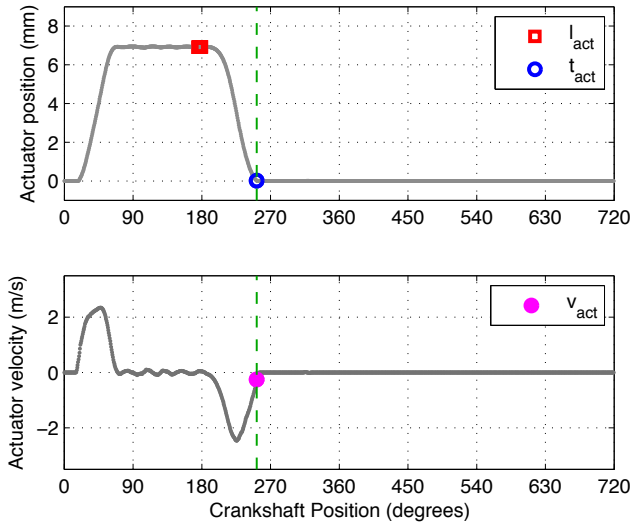

Fig. 4. Valve event performance parameters for a given cycle.

gain in real time to compensate for changes in the supply pressure.

B. Seating controller

The valve is considered to be seated at the instant at which the actuator crosses 0.1 mm going downward. This slight offset is used to ensure that the sensor noise does not affect the calculation of closing time. The crankshaft position (in CAD) at the time at which this crossing occurs is reported as the closing time. The actuator velocity is calculated by numerically differentiating the position data. The actuator velocity corresponding to the closing time is reported as the seating velocity. This is illustrated in Fig. 4.

The initial conditions of the IFS during valve closing will be disturbed by changes in valve lift. As the lift increases, the actuator velocity for the same triggering position will increase. This changing actuator velocity along with the on-off valve delay time will affect the seating behavior of the system. Hence, the on-off valve timing needs to be adjusted to compensate for these variations to ensure desired seating behavior. The three-way valve will also need to be adjusted to compensate for the varying amounts of time the engine valve will require to return from different lifts. Also, the engine valve takes a longer time to seat at lower seating velocities. The three-way valve off timing can be used to compensate for this effect as well.

The system exhibits an inherent tradeoff between seating velocity and variability in closing time. It can be seen in Fig. 6 that the variability in closing time increases as the seating velocity decreases and as lift increases. In general, the seating velocity is allowed to increase with engine speed, and since high lifts are required only for high engine speeds, the system will never operate in the high-variability regions on the plot. There is also an optimal point at each operating condition at which the seating velocity is as low as possible while maintaining the closing time variability near the system's inherent limit.

To identify that optimal operating point, an auxiliary

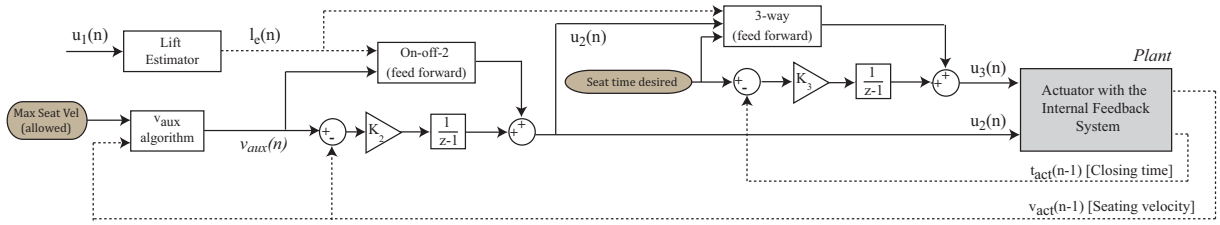

Fig. 5. Block diagram of the feed-forward + feedback controller for seating behavior

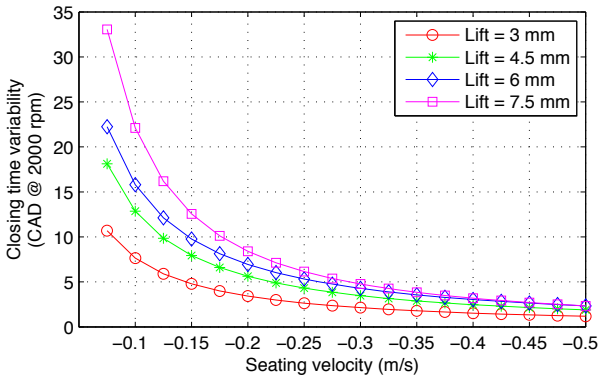

Fig. 6. Tradeoff between closing time variability and seating velocity. Variability is defined as the range of seating times over 11 consecutive cycles; the curves shown here are fit to the variability data.

variable (v_{aux}) for the desired seating velocity is calculated online and updated using the following equation:

$$\begin{aligned} v_{aux}(n) &= v_{aux}(n-1) + K_4 \times [v_{max,des}(n) - v_{max,act}(n-1)] \\ &\quad - K_5 \times [t_{range}(n-1)] \\ K_4 &= \begin{cases} 1/k & \text{if } v_{max,act}(n-1) < v_{max,des}(n) \\ 0 & \text{otherwise.} \end{cases} \\ K_5 &= \begin{cases} K_{t_{range}} & \text{if } t_{range}(n-1) > t_{range,min} \\ 0 & \text{otherwise,} \end{cases} \end{aligned} \tag{2}$$

where $v_{max,des}$ is the upper bound on seating velocity, $v_{max,act}$ is the maximum observed seating velocity over the last k cycles, t_{range} is the observed range in closing time over the last ten cycles, and $t_{range,min}$ is the threshold for the closing time variability below which the controller will not attempt to reduce the variation. Higher seating variability will tend to increase the value of v_{aux}, while any velocities above the desired threshold will act to decrease it. The value for k was chosen as 10, to minimize oscillation in v_{aux} while having the best possible transient response. Please note that all velocity values are negative, as seen on the x-axis of Fig. 6.

$K_{t_{range}}$ determines the rate of change of v_{aux} with respect to the observed closing time variability. A high value for $K_{t_{range}}$ can cause v_{aux} to oscillate undesirably, while a low value can result in a slow rate of reduction of the variability. Hence, it is determined experimentally to ensure that v_{aux} tunes itself to a value that ensures optimal closing time variability and sub-threshold seating velocity for each possible operating condition. The seating controller discussed below will then attempt to track this value of v_{aux}. This control architecture is more practical since the maximum velocity threshold can be set for each lift and engine speed to satisfy noise and wear concerns.

Fig. 5 shows the block diagram of the proposed seating controller that contains both feed-forward and feedback terms to compensate for the variation in initial conditions for the seating-side IFS due to lift variation and to account for the coupled effect of the closing time and seating velocity between the on-off and the three-way valves.

The control inputs are calculated using the following equations:

$$\begin{aligned} u_2(n) &= u_{2,fb}(n) + u_{2,ff}(n) \\ u_{2,fb}(n) &= u_{2,fb}(n-1) + K_2 \times [v_{aux}(n) - v_{act}(n-1)] \\ u_{2,ff}(n) &= \mathcal{FF}_2(l_e, v_{max,des}) \end{aligned} \tag{3}$$

$$\begin{aligned} u_3(n) &= u_{3,fb}(n) + u_{3,ff}(n) \\ u_{3,fb}(n) &= u_{3,fb}(n-1) + K_3 \times [t_{des}(n) - t_{act}(n-1)] \\ u_{3,ff}(n) &= t_{des}(n) - \mathcal{FF}_3(l_e, u_2(n)), \end{aligned} \tag{4}$$

where u_2 is the time (in CAD after the three-way valve is closed) or lift (in mm) at which on-off valve $\{2\}$ is closed, u_3 is the time (in CAD) at which the three way valve $\{3\}$ is closed, $u_{2,fb}$ and $u_{2,ff}$ are the feedback and feed-forward portions of the control input for on-off valve $\{2\}$, $u_{3,fb}$ and $u_{3,ff}$ are the feedback and feed-forward portions of the control input for the three-way valve $\{3\}$, K_2 and K_3 are the corresponding proportional learning gains. K_2 is chosen experimentally to enable v_{act} to effectively track v_{aux}. Since the relationship between u_3 and t_{act} is one-to-one, K_3 can be set to 1 CAD/CAD to ensure adequate tracking. $\mathcal{FF}(\cdot)$ is a polynomial surface mapping the inputs to the feed-forward output, $l_e(n)$ is an approximation of the lift for the current (n^{th}) cycle based on $u_1(n)$ as calculated by (1), and v and t are the performance parameters (desired and actual) seating velocity and closing time, respectively. Again, the indices n and $n-1$ are used to represent the current and previous cycles, respectively. The feed-forward surfaces were obtained by performing set-point tracking experiments at 2000 RPM. For other engine speeds, they can be scaled appropriately.

IV. Experimental Results

A compact multi-cylinder FFVA setup (Fig. 8) was used to test the developed control algorithm. The controller was implemented on only one of its valves, because little interaction was observed between valves of adjacent cylinders actuated 180 or 360 CAD out of phase over the range of engine speeds used in testing.

To obtain realistic trajectories for desired engine speed, lift, and closing time, a simulation of throttle-less load control over the Federal Test Procedure (FTP) driving cycle

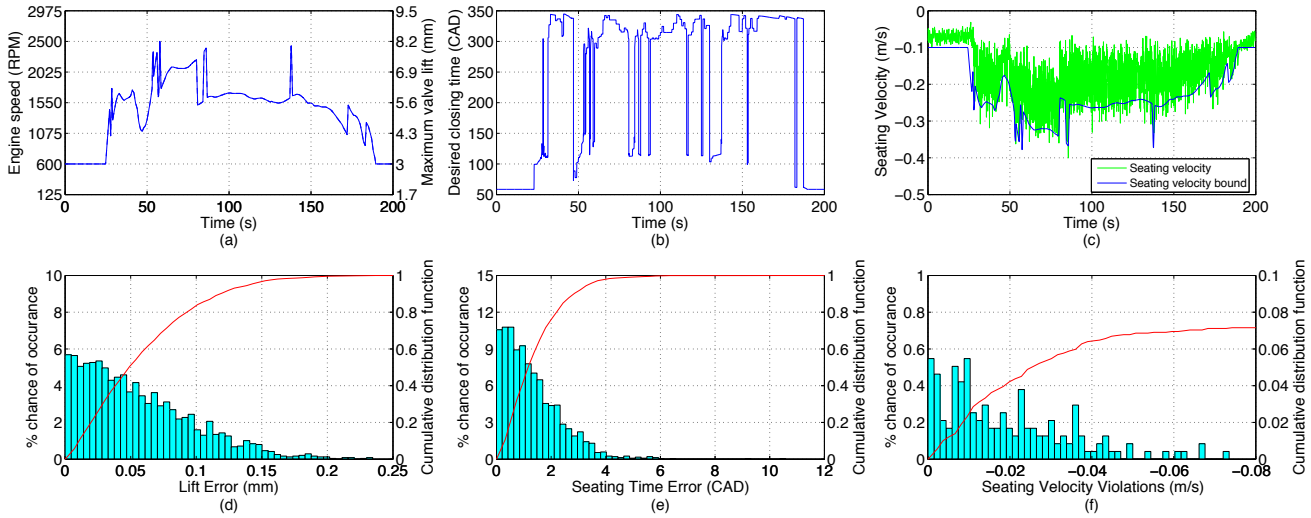

Fig. 7. RPM and desired lift (a), desired valve closing time (b), and seating velocity and seating velocity bound (c) trajectories, with lift error (d), closing time error (e), and seating velocity bound violation (f) statistics.

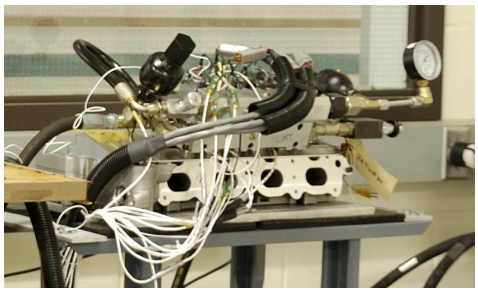

Fig. 8. Prototype experimental setup

was carried out. Data corresponding to tracking the most aggressive portion of the FTP cycle are presented here. The engine speed, valve lift, and seating velocity bound are linked proportionally, as shown in Fig. 7(a) and (c). Fig. 7(b) shows the desired closing time. Fig. 7(c) also shows the actual seating velocity. Fig. 7(d), (e), and (f) show the tracking error magnitude histograms and cumulative distributions for lift, closing time, and seating velocity, respectively. Note that Fig. 7(f) shows only those cycles with seating velocities higher than the desired bound (as any seating velocity below the bound is considered acceptable), but with probabilities normalized to the total number of cycles over the length of the test (2375 cycles).

Note that tracking of even very large (> 100 CAD) duration transients (see Fig. 7(b)) produces no noticeable disturbance in the tracking error in Fig. 7(e). Further note from the cumulative distributions in Fig. 7(d) and (e) that 99% of cycles have lift and closing time errors less than 0.183 mm and 4.71 CAD, respectively. Finally, seating velocity violations occur only 7.16% of the time, and the majority of those violations that do occur are relatively small in magnitude, as can be seen in Fig. 7(f).

V. Conclusion

An iterative learning controller has been designed for a fully-flexible valve actuation system. The internal feedback system has the benefit of simplifying the external controls. The proposed controller is able to track transients in desired lift and closing time with minimal violations of a maximum seating velocity constraint. The precise tracking performance allows cycle-to-cycle control of the profile characteristics (timing, lift, and duration) of individual engine valves, which in turn has benefits in engine power, efficiency, and advanced combustion control.

Acknowledgements

The authors would like to thank General Motors Research and Development for the hardware support.

References

[1] T. Hosaka and M. Hamazaki, "Development of the variable valve timing and lift (VTEC) engine for the Honda NSX," SAE Tech. Paper 910008, 1991.

[2] R. Flierl and M. Klüting, "The Third Generation of Valvetrains – New Variable Valvetrains for Throttle-Free Load Control," *SAE Technical Paper Series*, NO. 2000-01-1227, 2000.

[3] M. Fujiwara, K. Kumagai, M. Segawa, R. Sato, and Y. Tamura, "Development of a 6-Cylinder Gasoline Engine with New Variable Cylinder Management Technology," *SAE Technical Paper Series*, NO. 2008-01-0610, 2008.

[4] V. Picron, Y. Postel, E. Nicot, and D. Durrieu, "Electro-Magnetic Valve Actuation System: First Steps toward Mass Production," *SAE Technical Paper Series*, NO. 2008-01-1360, 2008.

[5] J.W.G. Turner, M.D. Bassett, R.J. Pearson G. Pitcher, and K.J. Douglas, "New Operating Strategies Afforded by Fully Variable Valve Trains," *SAE Technical Paper Series*, NO. 2004-01-1386, 2004.

[6] N. Milovanovic, R. Chen, and J. Turner, "Influence of the Variable Valve Timing Strategy on the Control of a Homogeneous Charge Compression (HCCI) Engine," *SAE Technical Paper Series*, NO. 2004-01-1899, 2004.

[7] W. Hoffmann, K. Peterson, and A.G. Stefanopoulou, "Iterative Learning Control for Soft Landing of Electromechanical Valve Actuator in Camless Engines," *IEEE Transactions on Control System Technology*, Vol. 11, No. 2, March 2003.

[8] Z. Sun and T.W. Kuo, "Transient Control of Electro-Hydraulic Fully Flexible Engine Valve Actuation System," *IEEE Transactions on Control System Technology*, Vol. 18, No. 3, May 2010.

[9] Z. Sun, "Electrohydraulic Fully Flexible Valve Actuation System With Internal Feedback," *ASME Journal of Dynamic Systems, Measurement, and Control*, Vol. 131, March 2009.

[10] Z. Sun, "Engine valve actuator assembly with dual automatic regulation," U.S. Patent 6 959 673 B2, Jan. 4, 2005.

[11] P. Gillella and Z. Sun, "Design, Modeling, and Control of a Camless Valve Actuation System With Internal Feedback," *IEEE/ASME Transactions on Mechatronics*, DOI 10.1109/TMECH.2010.2045656.

[12] D.A. Bristow, M. Tharayil, and A.G. Alleyne, "A Survey of Iterative Learning Control: A Learning-Based Method for High-Performance Tracking Control," *IEEE Control Systems Magazine*, June 2006.

[13] G. Oriolo, S. Panzieri, and G. Ulivi, "Cyclic Learning Control of Chained-Form Systems with Application to Car-Like Robots," *Proc. of 13th Triennial World Congress of IFAC*, 1996.